Mechanical Solutions to Variable Stiffness Robotic Arms

Xianpai Zeng[1], Tyler Morrison[2] and Hai-Jun Su[3]

***Abstract*— Collaborative robots or Co-robots are widely used in automotive industries and material handling. Co-robots are designed to work with human workers side by side. However, safety is a challenging major concern. Rigidity is required to carry a payload and achieve accuracy in motion, while flexibility is often required for safe human interaction. Robots with control over their stiffness could combine some of the advantages seen in compliant robots with the performance of traditional rigid robots. This paper aims at presenting several variable stiffness solutions developed in the Design, Innovation, and Simulation Laboratory (DISL) at The Ohio State University. These methods are classified based on the working principles and compared quantitatively based on the criteria such as stiffness range, stiffness ratio, and response time. Pros and cons are also described for each method.**

I. Introduction

Close cooperation between intelligent assistive robots and human workers could improve the efficiency of complex production processes. This cooperation involves physical human-robot interaction (pHRI) which requires deliberate design of production equipment around human operators [1]. Hybrid assembly – the process of robots and human workers jointly performing a handling and/or assembling task – is proven to have higher efficiency and lower cost compared to pure robotic or human assembly [2]. In order for co-robots to work safely and effectively alongside humans, flexibility and rigidity are both required. Flexible structures ensure safe human-robot interaction while rigidity is a critical design consideration for load carrying capability and high motion accuracy. Existing research shows that robotic arms designed with greater compliance are less likely to cause injury to humans [3], [4]. Some authors also argue that, through an effective control policy on stiffness variation, total operating time for a typical rest-to-rest task can be minimized by appropriately blending slow-and-stiff and fast-and-soft phases, [3], [5] but the variability and controllability of such compliance remains challenging [6].

Compliant robotics is an important frontier of co-robotic research. Compliant robots are typically constructed from materials such as textiles and elastomers, but can be made from any highly compliant material. Due to their compliant nature and theoretically infinite degrees of freedom, compliant robots can be extremely durable and more dexterous, and do not require careful control and environmental awareness to avoid damaging payloads or harming humans [7], [8].

Compliant robots can also be less expensive, lighter, and easier to customize for different applications when compared to traditional robots [9]. However, there are some limitations associated with the high compliance. One challenge with compliant robotics is maintaining high positional accuracy. The inherit flexibility makes it difficult to control the exact position of the soft robot's appendages. The theoretically infinite degrees of freedom makes applying traditional sensor setups such as encoders a challenge. Additionally, compliant robot tends to have large deformation under external load. This prevents compliant robots from matching the load-carrying capabilities and acceleration speeds of traditional rigid robots, which limits their potential uses.

Due to the performance limitations of compliant robots, there is interest in variable stiffness technologies. Robots with control over their stiffness could combine some of the advantages seen in compliant robots with the performance of traditional rigid robots. For example, a robot capable of varying its stiffness can become more rigid when higher positional accuracy or load capabilities are needed, but can also become more complaint to prevent injuring surrounding humans or damaging the environment. The additional safety that variable stiffness allows for is of increasing interest as robots which interact with humans become more common. For robots in assistive, rehabilitation, and domestic roles, safety is a critical design concern. This safety risk must be addressed before robots which work alongside humans can become more prevalent, and variable stiffness capabilities may be an important solution.

This work proposes a review of four variable stiffness concepts and six prototypes from the Design Innovation and Simulation Laboratory (DISL). Blanc *et al.* classified controllable stiffness mechanisms on the basis of intrinsic properties change [5]. The solution of the first main family is to change the second moment of the area, and the second main family's solution is to change the structure's elastic properties. This approach to classification and description is a major inspiration to our approach in this paper. Section II introduces a classification of the four concepts based on the underlying working principles including a summary of the design and experimental results for each concept. Section III gives a quantitative comparison.

This material is based upon work supported by the National Science Foundation under Grant No: CMMI-1637656. Any opinions, findings, and conclusions or recommendations expressed in this material are those of the author(s) and do not necessarily reflect the views of the funding agencies.

[1]Xianpai Zeng is with the Department of Mechanical & Aerospace Engineering, The Ohio State University,Columbus, OH 43210, USA. zeng.108@osu.edu

[2]Tyler Morrison is with the Department of Mechanical & Aerospace Engineering, The Ohio State University,Columbus, OH 43210, USA. morrison.730@osu.edu

[3]Hai-jun Su is with Faculty of the Department of Mechanical & Aerospace Engineering, The Ohio State University,Columbus, OH 43210, USA. su.298@osu.edu

II. Designs

A. Shape Morphing Cross-Section

1) Concept: The shape morphing concept varies stiffness by changing the cross-sectional shape of the beam. The prototype (SM1) proposed in [10] is comprised of a servo motor, four pairs of bearing frames, two universal transmission shafts, two flexible beams, and three cable-driven mechanisms as shown in Fig. 1. The flexible beams are the key concept for achieving variable lateral stiffness. In compliant mode, these beams relaxed and flat. In stiff mode, they are morphed into a curved shape which has a higher stiffness for lateral loads just as a sheet of paper can be folded to increase its stiffness.

The lateral stiffness of a single fixed-guided shape-morphing beam is

$$k = \frac{12EI}{L^3} \tag{1}$$

where E is the elastic modulus, L is the beam length, and I is the appropriate second moment of area of the cross-section. According to (1), changing I changes stiffness proportionally. To determine the required actuator position to achieve a given stiffness, the shape of the beam cross-section due to a deflection of its tip via the cable-driven mechanism can be determined by applying classical beam theory, and I can be determined by integrating the cross-section.

However, achieving variable stiffness is not useful if the device cannot support loads in other directions. Therefore, four prismatic bearing frames are added to connect the cable-driven mechanisms. The proximal cable-driven mechanism is fixed to the base housing and the distal cable-driven mechanism is attached to the end housing. The bearing frames are designed as a square rail with linear guides permitting prismatic extension and contraction, and the connections between the bearing frames and cable-driven mechanisms are rotational joints. As a result, the shape morphing arm behaves as a compliant parallel-guided mechanism in the lateral direction with variable stiffness while it remains rigid in the vertical direction and the perpendicular lateral direction.

In order to morph the flexible beams uniformly, three cable-driven mechanisms are distributed along the length of the morphing beams. To reduce the number of actuators, two universal transmission shafts are designed to couple the three cable-driven mechanisms such that a single servo motor in the base housing connected to the shaft can actuate all three cable-driven mechanisms simultaneously.

The center-line of the flexible beams is fixed to the cable-driven mechanisms, while the upper and lower edges of the flexible beams are connected to the transmission system with cables so that they are pulled inward and flexed into a concave shape (see Fig. 1(b)). The base housing, end housing, cable-driven mechanisms and bearing frames can be considered the rigid "skeleton," while the flexible arms are like "muscles."

2) Results: The prototype of this concept (SM1) is constructed from plastic with an elastic modulus of $1.2\,\mathrm{GPa}$. In its most compliant mode, the stiffness of the prototype

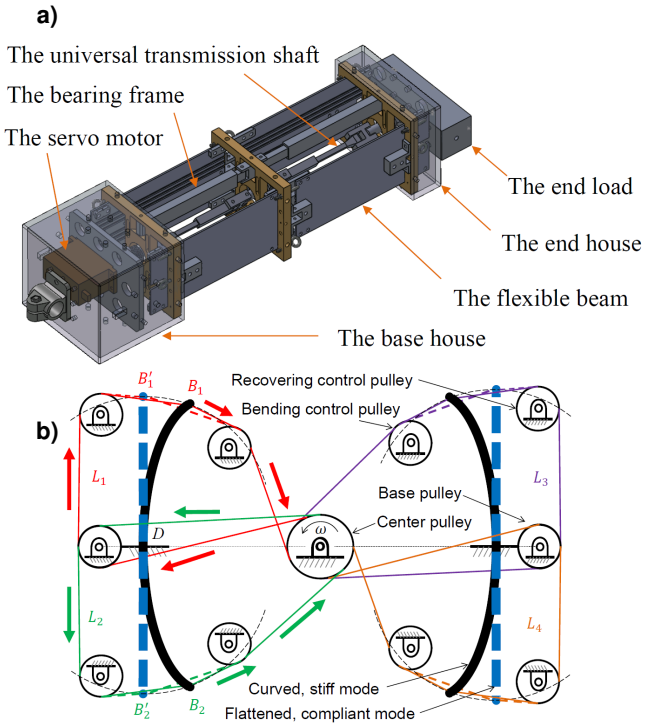

Fig. 1. (a) Prototype of the shape-morphing cross-section concept showing all components [10]. (b) Cross-section of one of the three sections of compliant mechanism used in the beam. A center pulley connected to the servo via the transmission shaft pulls a set of four cables that each flex the beam into a concave shape when activated.

is $0.207\,\mathrm{N/mm}$ while in its stiff mode, the stiffness is $0.458\,\mathrm{N/mm}$. This results in a stiffness ratio of 2.21. A pseudo-rigid-body model is proposed in [10] which accounts for the morphing angle of the cross-section and closely matches experimental results.

Another version of the same concept (SM2), shown in Fig. 2, is presented in [11]. In this work, the cable driven approach is replaced with a set of four-bar mechanisms. This beam, made from the same plastic, can vary lateral stiffness from $0.540\,\mathrm{N/mm}$ to $1.936\,\mathrm{N/mm}$ and therefore achieves a stiffness ratio of 3.6

3) Pros and Cons:

Pros

- *Control* — Control of the stiffness is easily obtained by modeling of the relationship between stiffness and morphing actuator angle, and closed loop control of morphing actuator.
- *Actuation Time* — Actuation is quick and is directly related to the power of the servo motor.
- *Scalability* — Scaling of the stiffness range of this design can be accomplished by changing the material selection, beam cross-section dimensions or length.

Cons

- *Mechanical Complexity* — The mechanical complexity of the linkage and transmission system needed to uniformly morph a beam introduces design and mass overhead and additional failure points.

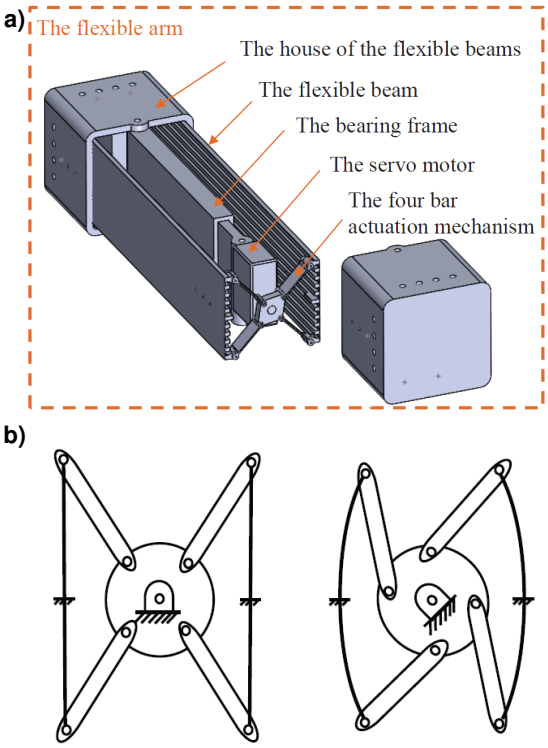

Fig. 2. (a) Prototype of the shape-morphing cross-section concept showing all components [11]. (b) Cross-section of one of the three sections of compliant mechanism used in the beam. A central mechanism pulls the edges of the beam inward into a concave shape.

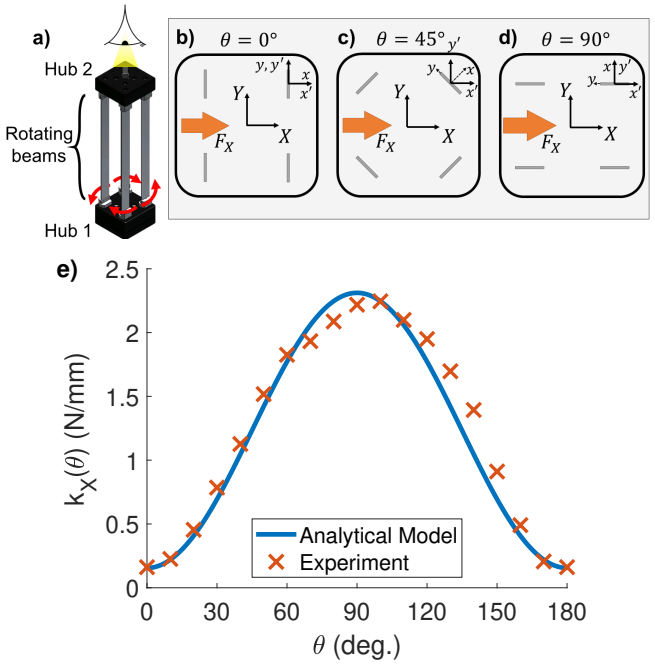

Fig. 3. (a) Illustration of the RBL concept [12] with sub-figures (b-d) showing the cross-section of the link from the top-down view. Four parallel beams form the structure of the link. When rotating the beams by θ in sync as in from (b) to (c) and (c) to (d), their alignment with the lateral load F_X changes the effective area moment of inertia and therefore the resulting lateral stiffness. (e) The link lateral stiffness as a function of beam angle.

- *Actuator Effort* — Even without the presence of an external load, the actuators need to exert a force/torque to hold the beam in its morphed shape.

B. The Rotating Beam Link (RBL)

1) Concept: Fig. 3 shows an overview of the prototype design of the rotating beam link (RBL). Four parallel thin aluminum beams are joined at each end to a hub which contains a gearbox for rotating the beams with the servo in each hub. This design is motivated by considering the transformation of area moments of inertia under rotation by θ from the beam-fixed x-y frame to the link-fixed x'-y' frame centered on the beam. For a symmetric beam with a rectangular cross-section and the x-y coordinate system at its centroid, $I_{xy} = 0$ and

$$I_{y'} = \frac{I_x + I_y}{2} - \frac{I_x - I_y}{2}\cos(2\theta)\,. \tag{2}$$

where I_x and I_y are the area moments of inertia in the rotating frame and $I_{y'}$ is an area moment of inertia in the fixed frame.

If we assume that $I_x > I_y$ as indicated by Fig. 3, intuitively, (2) has minima at the angles $\theta = j\pi$, and maxima at the angles $\theta = (\pi/2 + j\pi)\,, \quad \forall j \in \mathbb{Z}$. As a result, we can vary the lateral stiffness as a sinusoid by symmetrically rotating the beams.

2) Results: In [12], we demonstrate a prototype of our new variable stiffness link concept achieves a stiffness ratio of 13.9 between its extreme positions, and a ratio of 8.6 between its neutral configuration and its compliant configuration. However, this is a significant difference from the ideal theoretical ratio of the prototype which is shown to be 122. The difference in these ratios is due to parasitic compliance introduced by the components in the drive-train that are necessary to actuate the rotating beams.

Finite element analysis suggests the maximum torsional stiffness of the link is about $19\,\mathrm{N\text{-}m/rad}$, and experimental tests show the link can support $20\,\mathrm{N}$ of axial compression without buckling, and substantially more at other beam angles. If necessary, torsional load capacity may be improved by adding an extra mechanism between the two hubs of the robotic arm.

The model we developed for the lateral stiffness of the link as a function of the beam angles includes a complete accounting of the compliance in each beam as well as buckling phenomena and it accurately predicts stiffness behavior of the prototype. We also show that the model can be used to help characterize the effect of parasitic compliance: an essential challenge of implementing this concept into a working design.

3) Pros and Cons:

Pros

- *Control* — Control of the stiffness ratio is easily obtained by modeling of the relationship between stiffness and beam angle, and closed loop control of beam angle.

- *Actuator Effort* — Actuator effort to maintain a stiffness is only required under external loads.
- *Actuation Time* — Actuation is quick. Beams only need to rotate 90 degrees to obtain largest stiffness change.
- *Scalability* — Scaling the stiffness ratio and range of the design can be accomplished by changing material selection, beam cross-section dimensions, beam length, or number of beams.

Cons

- *Mechanical Complexity* — The mechanical complexity of the transmission system adds mass overhead and introduces parasitic compliance which decreases stiffness throttling performance.
- *Buckling* — The reliance of the design on several long, slender beams introduces an opportunity for elastic buckling in certain loading modes which decreases stiffness performance and induces non-linearities which impede modeling.

C. Slider on Parallel-Guided Arm

1) Concept: The slider variable stiffness robotic arm is based on a parallel guided beam, and consists of two end-guided flexures with a rigid connection in between. The stiffness of the arm is calculated as:

$$k = \frac{24EI}{L^3} \tag{3}$$

where, E is the elastic modulus of the beam material, I is the cross-section area moment of inertia of each sheet, and L is the effective beam length. The concept of the design is to change the effective length of the parallel guided beam to implement stiffness variation.

The first prototype based on this concept is shown in Fig. 4 [13]. The stiffness change is enabled by changing the effective length of beams through a roller carriage which is actuated by a screw drive and an electric motor. The arm has two parallel Al 7075 sheet flexures. The fixed end is designed to be the motor and transmission housing. A power screw is assembled through the slider. To allow the bending of the two flexures, a small nut featuring with grooves is added to the free end containing spherical balls as rolling supports. As the carriage is moved towards the free end, the free length of the flexures decreases, leading to an increase in stiffness since the support bar has high stiffness. The overall dimensions of the prototype are $406\,\mathrm{mm} \times 95\,\mathrm{mm} \times 104\,\mathrm{mm}$ and the total weight is $952\,\mathrm{g}$.

Fig. 5 [14] shows the second prototype which is based on the same concept. A low-weight, high-speed pneumatic cylinder is used to decrease the time of stiffness variation. The carriage runs along the support bar, with linear bearings to reduce friction. It makes contact with the actuator only in the axial direction, and the bar carries all lateral loads. The boundary conditions are enforced using roller bearings that make contact with the sheets. The free ends of the sheet flexures are connected by a single part, which is then allowed to move with respect to the cylinder by rolling contact through metal balls. The overall dimensions of the

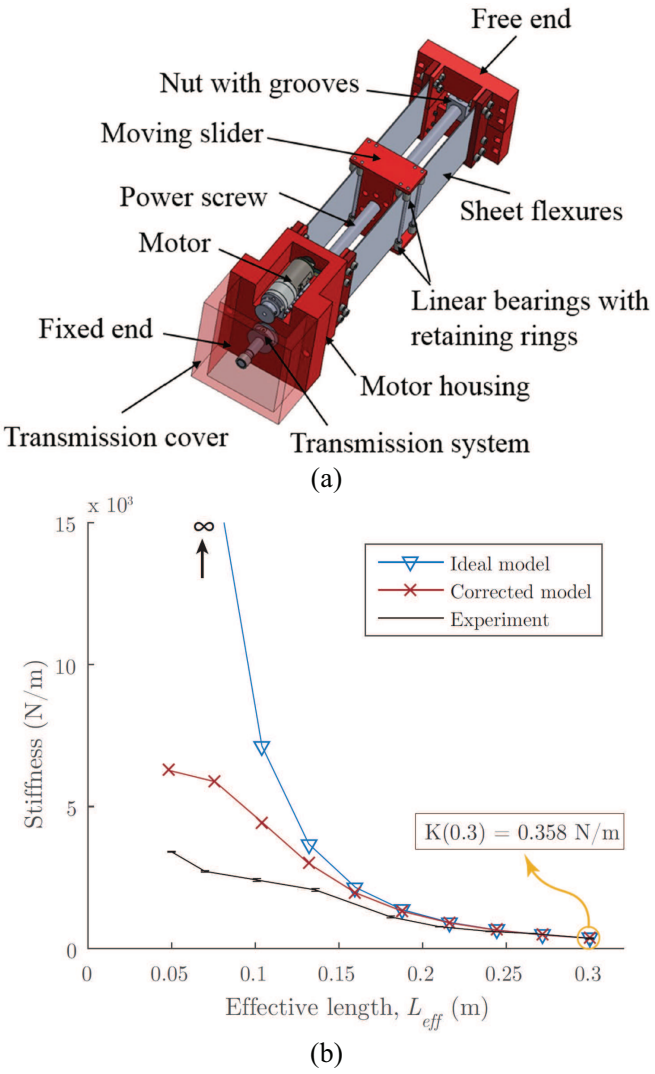

Fig. 4. (a) Prototype of the parallel-guided arm with screw driven slider [13]. (b) Link stiffness as a function of effective length for the design with screw and motor driven slider.

arm are $450\,\mathrm{mm} \times 100\,\mathrm{mm} \times 100\,\mathrm{mm}$. The total mass is $450\,\mathrm{g}$.

2) Results: The link with the slider actuated by motor and screw drive is capable of stiffness change by 20 fold, with the maximum static stiffness at $10.049\,\mathrm{N/mm}$ and the minimum value at $0.500\,\mathrm{N/mm}$. The link with the slider actuated by pneumatic cylinder could achieve a relatively low stiffness change of 10 fold, but it can be achieved in $0.6\,\mathrm{s}$. The maximum stiffness is $3.407\,\mathrm{N/mm}$ and the minimum stiffness is $0.358\,\mathrm{N/mm}$.

3) Pros and Cons:

Pros

- *Payload* — High load capacity is obtained due to the parallel-guided configuration.
- *Stiffness Range (Screw Driven)* — For the design that uses the screw driven slider, very large stiffness range is feasible. The power screw shaft has very large stiffness

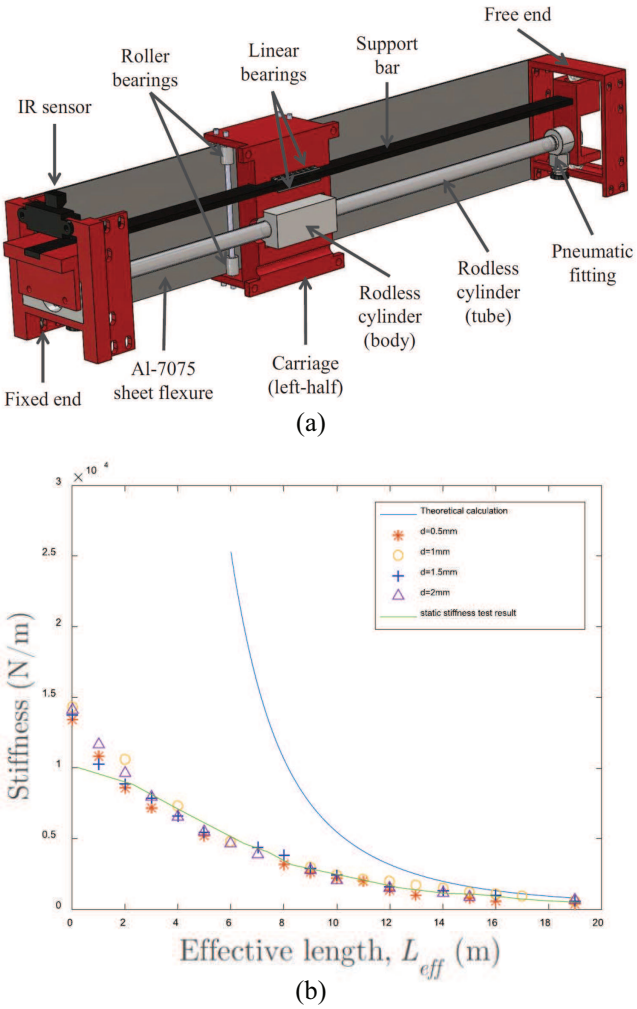

Fig. 5. (a) Prototype of the parallel-guided arm with pneumatic cylinder driven slider [14]. (b) Link stiffness as a function of effective length for the design with pneumatic cylinder driven slider.

which adds to the overall stiffness significantly when fully coupled with the parallel-guided beam.

- *Response (Pneumatic Driven)* — The effective length can be changed quickly since the slider can move very fast when driven with the pneumatic cylinder.
- *Control* — Control of the stiffness is directly related with the effective beam length.

Cons

- *Response (Screw Driven)* — The moving speed of the slider driven with screw and motor is related to the screw pitch, motor power. Motors with higher power tend to be bulky and expensive which limits the overall response time, and adds mass to the link.
- *Actuator Effort* — Extra actuator effort is needed to move the slider while the link is deflected.

D. Layer Jamming on Parallel-Guided Arm

1) Concept: This section introduces a parallel-guided robotic arm that can achieve a large stiffness variation ratio – up to 75 times – through pneumatic actuated layer jamming [15]. Fig. 6 (a) illustrates the basic configuration of the parallel-guided arm. The robotic arm is composed of two 3D printed flexible beams securely clamped on both ends. Juxtaposing two beams in parallel makes the robotic arm more resilient to bending moments due to the end constraints and results in a higher vertical load capability compared to a single beam. A novel cross-section that features interconnected stiff and soft sections is proposed. As illustrated in Fig. 6 (b), the hourglass shaped stiff sections are connected through the relatively longer and thinner soft sections. With this novel design, the beam has large thickness but retains high flexibility. Fig. 6 (c) illustrates the interleaved arrangement of jamming layers. On both sides of the beam, jamming layers are laid on top of the hourglass shaped sections. One group of layers, shown in green, is bonded to the left end of the beam, the other group of layers, shown in yellow, is attached to the right end. The two groups are shuffled evenly so that the layers are on top of each other. The effect of layer jamming is augmented by the enhanced beam thickness due to the increased leverage of friction force exerted by the jammed layers.

2) Results: Force and deflection data have been collected while the arm is deflecting from its initial position to a tip deflection of $20\,\mathrm{mm}$. Multiple data collections are made from 0 psig to 12.5 psig with an increment of 2.5 psig. Experimental result is presented in Fig. 7. For a given vacuum pressure, the stiffness of the parallel-guided arm initially increases linearly followed by a non-linear increase phase, in which the rate of increase starts to slow down. And finally the stiffness comes to saturate as the tip deflection reaches $20\,\mathrm{mm}$. During the unloading process, the arm tends to restore its initial position due the strain energy stored in the flexible backbone.

At 0 psig vacuum pressure, the arm stiffness is defined as the base stiffness which is used as the denominator to calculate stiffness variation ratio. The base stiffness characterizes the flexibility of the center backbone. Stiffness increases as the applied vacuum pressure is increased. The stiffness variation ratio is calculated as the stiffness corresponding to 12.5 psig divided by the base stiffness. Experiment on the prototype shows that a stiffness ratio of 75 is achieved. The minimum stiffness and maximum stiffness are $0.0803\,\mathrm{N/mm}$ and $6.05\,\mathrm{N/mm}$ respectively.

Quick actuation of the jamming layers is also an important design consideration. To remove the air from the vacuum bag in a quick manner, channels as an internal feature of beams have been designed to facilitate fast air removal. The internal air channels are made during the 3D printing, with no extra fabrication process needed. The other measure for generating vacuum quickly is to use vacuum generator rather than vacuum pumps. The flow rate of regular motor-based vacuum pumps is usually around 2 cfm (cubic feet per minute), with a few up to 10 cfm. However, air-powered vacuum generators can go up to 30 cfm. This significantly enhance the performance on adjusting the vacuum level. The jamming layers can be fully actuated in 0.25 second.

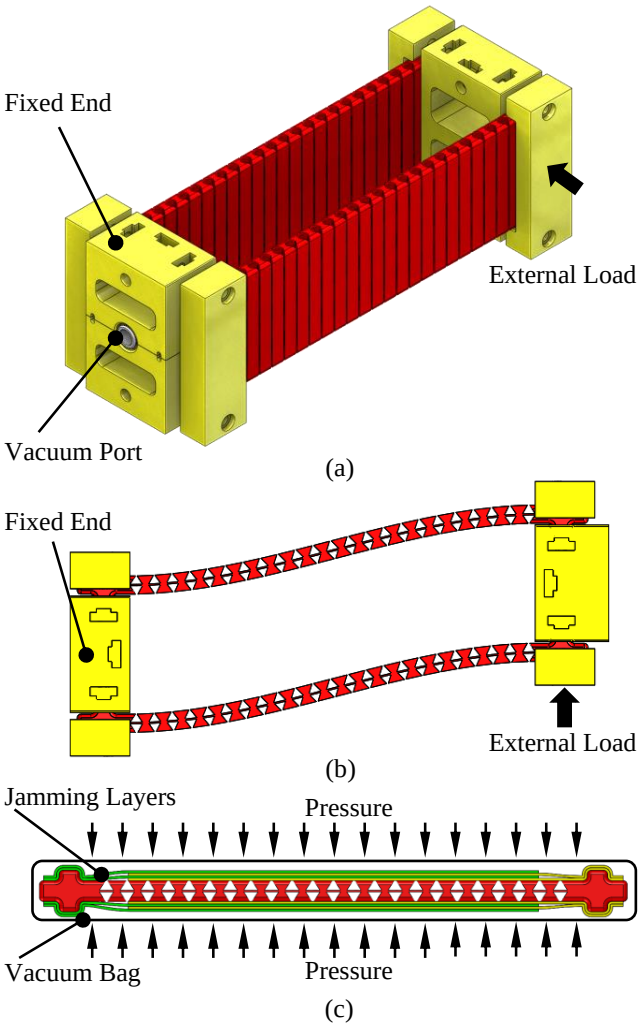

Fig. 6. Design concept of the parallel-guided arm with layer jamming [15]. (a) Basic configuration. (b) Deformed parallel-guided arm with one end fixed while the other moving laterally under external load. (c) Configuration of the vacuum membrane and jamming layers.

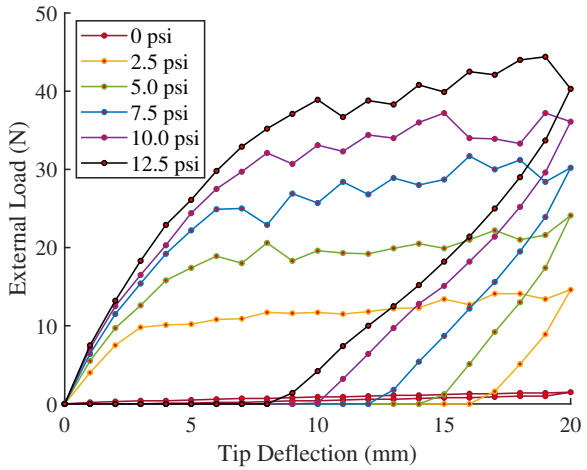

Fig. 7. Load-deflection measurement of the parallel-guided arm with layer jamming [15].

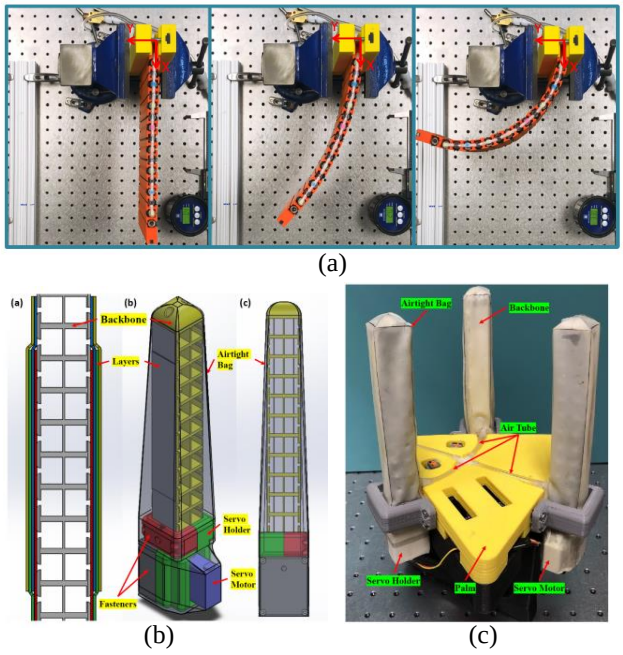

Fig. 8. Applications of layer jamming on (a) morphing structure with tunable stiffness [16] and (b) robotic gripper with variable stiffness [17].

Layer jamming for variable stiffness has also been applied to morphing structures and robotic grippers. Fig. 8 (a) shows a prototype [16] that is capable of both morphing its curvature and varying its stiffness. The structure is actuated via pneumatic air muscles to achieve high levels of curvature. Integrating the McKibben actuators inside the 3D printed structure allows this design to achieve much higher loading forces compared to previous morphing structures in soft robotics. In addition, this design achieved a maximum stiffness variation of 75 times. Fig. 8 (b) and (c) present a robotic grasper [17] with tunable stiffness by combining layer jamming with a cable-driven compliant mechanism. The stiffness and load capacity of the gripper are greatly increased. A 24-fold and 30-fold increase are observed respectively.

3) Pros and Cons:

Pros

- *Payload* — High load capacity is obtained due to the parallel-guided configuration.
- *Mechanical Complexity* — The design is simple and compact with few moving parts.
- *Response* — Specific design and part selection is used to facilitate fast air removal and vacuum pressure regulation.
- *Scalability* — Stiffness range and ratio could be varied by changing the beam dimensions, layers materials and number of jamming layers.

Cons

- *Modeling* — Analytical model for unloading is difficult due to the presence of hysteresis.

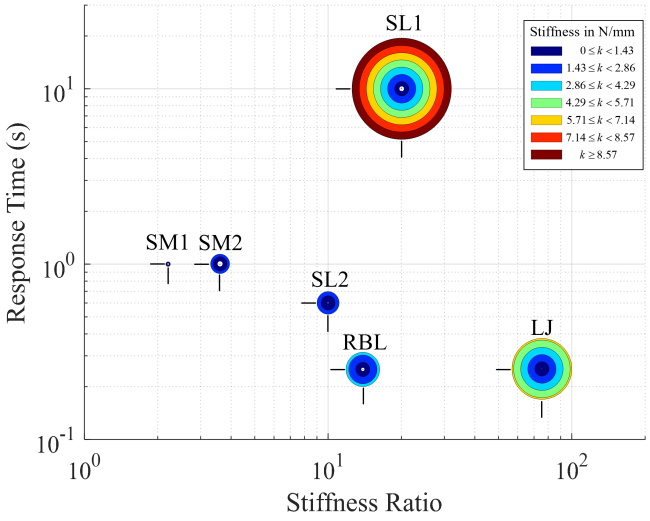

Fig. 9. Comparison of the stiffness ratio, stiffness range and response time for tunable stiffness solutions.

- *Control* — Due to the use of high flow rate vacuum generator, sophisticated pressure control algorithm and hardware are required.

III. Discussions

In Table I, each method is classified, and various properties are quantified. Fig. 9 gives a visual overview of the relative strengths and weaknesses of each approach in terms of stiffness and response time. It should be noted that not all design parameters are held constant between the various prototypes. Mass, length, material properties, etc., all vary somewhat between the devices which affects their variable stiffness performance and makes them difficult to compare. However, we can still draw some broad conclusions.

Consider the response time of the various methods. The shape morphing, rotating beam, pneumatic cylinder driven slider, and layer jamming designs have the advantage of a relatively quick response. The motors of the shape morphing and rotating beam links drive the mechanical actuation mechanism through cables, linkages or gears. With the selection of sufficient motors and driving mechanisms, response time could be further optimized. However, increasing the complexity of the driving mechanisms can have a negative impact on the stiffness ratio and mass. The pneumatic cylinder driven slider and layer jamming concepts have a relatively simpler configuration in terms of the number of moving parts and compactness. The pneumatic cylinder driven slider moves much faster than the screw driven slider on the linear guide thus achieving a significant performance gain at the cost of more extensive work on control and calibration. The response time of the layer jamming method is related to the amount of air that needs to be removed, the resistance in the fluid system, and the pump performance. The proposed layer jamming link optimizes the response time by using a tight vacuum bag, embedding internal air channels, and using a high flow rate vacuum generator. Achieving fast and precise pressure regulation also requires effort designing the control scheme.

Among the presented methods, the best stiffness ratio is attained by the layer jamming link. This is a result of both the relatively higher maximum stiffness – with no losses to parasitic compliance in any mechanical linkages – and the low minimum stiffness. The stiffness ratio of the layer jamming link depends on the beam dimensions, material selection of both the beam and jamming layer, number of layers, and available vacuum level. To design for maximum stiffness ratio, a comprehensive analytical model and extensive experiment are necessary. The links based on morphing shape require high wire tension or linkage bending stress to achieve high stiffness ratio. The rotating beam link has potential for much higher stiffness change, but design for a more secure beam boundary condition remains challenging. The links based on effective length change using sliders also need to improve the slider mechanism to provide large and secure clamping force on the beams.

Finally, the layer jamming approach has a unique benefit. It can change the stiffness while the link is deflected under external load by simply increasing or decreasing the vacuum pressure. Other links have more difficulty changing stiffness under external load. The wire and linkage driven mechanisms and the servo motor on the rotating beam link need larger motor torque to deform or actuate their pre-loaded beams. Similarly, a slider that moves on a deflected parallel-guided beam will have to overcome larger resistance.

IV. Conclusions

As in all engineering problems, the best variable stiffness design depends on the problem objectives and technical constraints. This paper gives an overview of several candidate designs based on the concept of varying the stiffness of the structure of what would otherwise be a rigid link. These designs are prototypes. Additional work is necessary to turn each of them into a mature technology, but many show promise. The layer jamming approaches have a high stiffness ratio and range and a fast response at the cost of implementing pneumatic pressure control. The slider approache with screw drive is simple but have slower response time. The other slider method with pneumatic driven slider is quick but need complex control algorithm. The variable cross-section based approaches have good stiffness ratios and response times, but suffer from mechanical complexity.

Promising future work involves implementing one or more of these concepts to solve a practical engineering problem with variable stiffness, such as multiple-section robotic arms, and iterating to improve the prototype designs and performance.

References

[1] H. Bley, G. Reinhart, G. Seliger, M. Bernardi, and T. Korne, "Appropriate Human Involvement in Assembly and Disassembly," *CIRP Annals*, vol. 53, no. 2, pp. 487–509, 2004. [Online]. Available: https://linkinghub.elsevier.com/retrieve/pii/S0007850607600262

TABLE I

COMPARISON OF PRESENTED VARIABLE STIFFNESS METHODS

Classification			Acronym	Prototype Properties				References
				Stiffness Ratio[1]	Actuation Time[2]	Stiffness Range (N/mm)	Modeling Difficulty	
Change in geometry	Cross-section	Shape morphing	SM1	2.2	<1 s	0.207 to 0.458	medium	Sec. II-A, [10]
			SM2	3.6	<1 s	0.540 to 1.936	medium	Sec. II-A, [11]
		Rotating beam link	RBL	122 (ideal) 13.9 (prototype)	<0.25 s	0.1613 to 2.245	medium	Sec. II-B, [12]
	Beam length	Sliding beam	SL1	20	10 s	0.500 to 10.049	easy	Sec. II-C, [13]
			SL2	10	0.6 s	0.358 to 3.407	easy	Sec. II-C, [14]
Change in elastic properties	Structural Interactions	Layer jamming	LJ	75	0.25 s	0.0803 to 6.05	difficult	Sec. II-D, [15]

[1]Stiffness ratio is defined as the ratio of maximum lateral stiffness to minimum lateral stiffness.
[2]Actuation time is defined as the time necessary to actuate from the maximum stiffness to the minimum stiffness.

[2] J. Krüger, T. Lien, and A. Verl, "Cooperation of human and machines in assembly lines," *CIRP Annals*, vol. 58, no. 2, pp. 628–646, 2009. [Online]. Available: https://linkinghub.elsevier.com/retrieve/pii/S0007850609001760

[3] A. Bicchi and G. Tonietti, "Fast and "Soft-Arm" Tactics," *IEEE Robotics & Automation Magazine*, vol. 11, no. 2, pp. 22–33, June 2004. [Online]. Available: http://ieeexplore.ieee.org/document/1310939/

[4] A. Bicchi, G. Tonietti, and R. Schiavi, "Safe and fast actuators for machines interacting with humans," in *IEEE Conference on Robotics and Automation, 2004. TExCRA Technical Exhibition Based.* Minato-ku, Tokyo Japan: IEEE, 2004, pp. 17–18. [Online]. Available: http://ieeexplore.ieee.org/document/1424973/

[5] L. Blanc, A. Delchambre, and P. Lambert, "Flexible Medical Devices: Review of Controllable Stiffness Solutions," *Actuators*, vol. 6, no. 3, p. 23, Sept. 2017. [Online]. Available: https://www.mdpi.com/2076-0825/6/3/23

[6] M. Manti, V. Cacucciolo, and M. Cianchetti, "Stiffening in Soft Robotics: A Review of the State of the Art," *IEEE Robotics & Automation Magazine*, vol. 23, no. 3, pp. 93–106, Sept. 2016. [Online]. Available: http://ieeexplore.ieee.org/document/7565718/

[7] D. Rus and M. T. Tolley, "Design, fabrication and control of soft robots," *Nature*, vol. 521, no. 7553, pp. 467–475, May 2015. [Online]. Available: http://www.nature.com/articles/nature14543

[8] D. Trivedi, C. D. Rahn, W. M. Kier, and I. D. Walker, "Soft robotics: Biological inspiration, state of the art, and future research," *Applied Bionics and Biomechanics*, vol. 5, no. 3, pp. 99–117, Dec. 2008. [Online]. Available: http://content.iospress.com/doi/10.1080/11762320802557865

[9] R. Wood and C. Walsh, "Smaller, Softer, Safer, Smarter Robots," *Science Translational Medicine*, vol. 5, no. 210, pp. 210ed19–210ed19, Nov. 2013. [Online]. Available: http://stm.sciencemag.org/cgi/doi/10.1126/scitranslmed.3006949

[10] Y. She, "A Continuously Tunable Stiffness Arm with Cable-Driven Mechanisms for Safe Human-Robot Interactions," 2019.

[11] Y. She, H.-J. Su, C. Lai, and D. Meng, "Design and Prototype of a Tunable Stiffness Arm for Safe Human-Robot Interaction," in *Volume 5B: 40th Mechanisms and Robotics Conference*. Charlotte, North Carolina, USA: ASME, Aug. 2016, p. V05BT07A063. [Online]. Available: http://doi.org/10.1115/DETC2016-59523

[12] T. Morrison, C. Li, X. Pei, and H.-j. Su, "A Novel Rotating Beam Link for Variable Stiffness Robotic Arms," in *2019 IEEE International Conference on Robotics and Automation (ICRA)*, Montreal, Canada, 2019, accepted.

[13] R. Hu, V. Venkiteswaran, and H.-J. Su, "A Variable Stiffness Robotic Arm Using Linearly Actuated Compliant Parallel Guided Mechanism," in *Mechanism Design for Robotics*, A. Gasparetto and M. Ceccarelli, Eds. Cham: Springer International Publishing, 2019, vol. 66, pp. 33–40.

[14] V. K. Venkiteswaran, R. Hu, and H. Su, "A Pneumatically-Actuated Variable-Stiffness Robot Arm Using Parallel Flexures," in *2018 IEEE International Conference on Robotics and Biomimetics (ROBIO)*. Kuala Lumpur, Malaysia: IEEE, Dec. 2018, pp. 1–7. [Online]. Available: https://ieeexplore.ieee.org/document/8665208/

[15] Z. Xianpai, C. Hurd, H.-j. Su, S. Song, and J. Wang, "A parallel-guided robotic arm with variable stiffness through mechanical layer jamming," *IEEE Transactions on Robotics*, 2019, under Review.

[16] C. Mikol and H.-j. Su, "An Actively Controlled Variable Stiffness Structure via Layer Jamming and Pneumatic Actuation," in *2019 International Conference on Robotics and Automation (ICRA)*, 2019, accepted.

[17] Y. Gao, X. Huang, I. S. Mann, and H.-j. Su, "A Variable Stiffness Comliant Robotic Gripper Based on Layer Jamming," in *ASME 2019 International Design Engineering Technical Conferences & Computers and Information in Engineering Conference (IDETC/CIE)*, 2019, submitted.